Research on Engineering Structures & Materials
www.jresm.org
MIM Research Group

Research Article

Experimental investigations on tensile and fracture behaviors of steel fiber-reinforced self-compacting concrete

Huayan Yao [1,2,a], Guangyu Zhou [2,b], Fan Yang [*,2,c], Hua Lu [1,d], Xingqi Zhang [3,e]

[1]*North Minzu University, Yinchuan, China*
[2]*School of Civil Engineering, Hefei University of Technology, Hefei, China*
[3]*Hefei Municipal Design and Research Institute Co., Ltd., Hefei, China*

Article Info

Article History:

Received 06 Nov 2025
Accepted 19 Mar 2026

Keywords:
Steel fiber;
Self-compacting concrete;
Brazilian disc splitting test;
Notched semi-circular bending test;
Fracture toughness

Abstract

To investigate steel fiber's influence on self-compacting concrete (SCC)'s tensile and fracture properties, Brazilian disc splitting and Notched Semi-Circular Bending (NSCB) tests were conducted. The effects of steel fiber length, diameter, and volume fraction on SCC's tensile strength and fracture toughness, as well as the correlation between the two properties in steel fiber-reinforced SCC (SFRSCC), were analyzed. Results show: tensile strength first increased then decreased with rising fiber length, diameter, and volume fraction; fracture toughness first rose then fell with length and diameter but increased continuously with volume fraction. Steel fiber volume fraction had a more significant impact on NSCB's secondary bearing stage than length or diameter. A significant linear relationship was found between the tensile strength and fracture toughness of SFRSCC.

1. Introduction

Self-compacting Concrete (SCC) has emerged as one of the most extensively utilized materials in the construction industry in recent years, owing to its high workability and self-compacting characteristics that eliminate the need for external vibration [1,2]. However, despite its numerous advantages, SCC exhibits limitations in mechanical strength, formability, and crack resistance [3,4]. Consequently, the incorporation of steel fibers into self-compacting concrete (SCC) has been proposed to enhance its material properties.

Steel fibers, known for their high stiffness and tensile strength, effectively bridge both micro-cracks and macro-cracks during the post-cracking phase of concrete. Consequently, incorporating appropriate amounts of steel fibers into concrete can enhance its mechanical properties [5]. Abbas et al. [6] investigated the influence of steel fiber length on the 28-day splitting tensile strength of concrete, demonstrating a superior enhancement with 8-mm fibers. Shi et al. [7] conducted uniaxial tensile tests on cylindrical specimens incorporating hooked-end and straight steel fibers, revealing that the tensile strength initially increased and then plateaued with rising volume fractions. Notably, straight fibers exhibited a greater strength increment than hooked-end fibers. However, with regard to the mechanical behavior, toughness, and flexural performance of concrete after cracking, end-hooked steel fibers have been widely demonstrated to provide better reinforcing efficiency than straight steel fibers due to their distinctive mechanical anchoring effect [8].Ning et al. [9] reported that steel fiber volume fractions of 0.38% and 0.64% significantly

*Corresponding author: fyang@hfut.edu.cn
[a]orcid.org/0000-0001-5199-6117; [b]orcid.org/0000-0003-2779-5707; [c]orcid.org/0000-0002-6532-8619; [d]orcid.org/0000-0001-5968-9736; [e]orcid.org/ 0000-0003-4770-3021
DOI: http://dx.doi.org/10.17515/resm2026-1324me1106rs

reduced the maximum crack width and average crack spacing in SCC beams, with the fiber aspect ratio having a pronounced effect on crack dimensions. Liu [10] assessed the mechanical properties of steel fiber-reinforced concrete through axial compression, residual flexural tensile strength, and flexural beam tests, confirming significant improvements in compressive and tensile strength compared to plain concrete. Han et al. [11] demonstrated that steel fibers effectively retard crack propagation, enhance the peak strain of SCC, and significantly improve compressive toughness in a dosage-dependent manner, while concurrently reducing workability due to increased internal frictional resistance. Li et al. [12] demonstrated that incorporating steel fibers effectively enhances the mechanical properties of SCC while concurrently optimizing its meso- and micro-pore structure. Ola [13] observed that excessive volumes of steel fiber may reduce tensile and compressive strength but still enhance crack resistance. Studies have shown that steel fiber-reinforced self-compacting concrete (SFRSCC) exhibits superior tensile and flexural properties compared with conventional vibrated steel fiber-reinforced concrete. This is mainly attributed to the crack-bridging effect of steel fibers [14]. The splitting tensile strength of self-compacting concrete with a steel fiber volume fraction of 0.75% can reach 4.12 MPa, which is 1.67 times that of ordinary steel fiber-reinforced concrete (2.47 MPa) [15]. It is evident that existing research predominantly focuses on conventional steel fiber-reinforced concrete (SFRC), which is prone to issues such as insufficient compaction, fiber clustering, or sedimentation during construction, thereby compromising structural performance. In contrast, steel fiber-reinforced self-compacting concrete (SFRSCC) eliminates the need for vibration due to its superior fluidity and self-consolidating characteristics, offering significant advantages in both construction efficiency and performance. Current studies and applications of SFRSCC remain limited, particularly regarding the comprehensive characterization of its tensile behavior and fracture mechanisms, which warrants further in-depth investigation. Fracture toughness is a fundamental parameter for analyzing the fracture behavior of concrete [16]. Therefore, research on fracture toughness is essential for understanding concrete fracture mechanisms. Current methods for determining fracture toughness include the Notched Semi-Circular Bending (NSCB) test [17], which has gained wide acceptance due to its simplicity in specimen preparation and testing apparatus [18,19]. However, this method has not been systematically applied to examine the fracture toughness of SFRSCC.

In this study, the tensile strength of SFRSCC with varying steel fiber lengths, diameters, and volume fractions was determined via Brazilian disc splitting tests. The load-displacement curve characteristics and failure modes of specimens were analyzed during this process. Utilizing NSCB tests, the effects of fiber geometric parameters on SCC fracture toughness were examined, alongside the load-displacement curve features and failure characteristics under NSCB conditions. Furthermore, a functional relationship between the fracture toughness and the tensile strength in SFRSCC was established through fitting analysis, providing a reference for engineering applications of SFRSCC.

2 Experiment Materials and Methods

2.1 Raw Materials

The raw materials comprised cement, fly ash, slag powder, water, a superplasticizer, coarse aggregates (including fine stones), fine aggregates (including fine sand and river sand), and hooked-end steel fibers. Fig. 1 illustrates different steel fibers, and their specifications are detailed in Table 1.

Table 1. Mechanical and geometric characteristics of hooked-end steel fibers

Length (mm)	Diameter (mm)	Tensile strength (MPa)	Modulus of elasticity (GPa)
25	0.80		
30	0.70		
30	0.80	1200	200
35	0.55		
35	0.70		

35	0.80

Fig. 1. Steel fibers with different characteristic parameters

2.2 Specimen Preparations

A C50 self-compacting concrete mix proportion was adopted as the baseline for preparing concrete specimens, with the proportion of mixture provided in Table 2. A total of 10 groups of specimens were designed in the test. The steel fiber parameters were selected in accordance with the Technical Specification for Application of Fiber Reinforced Concrete (JGJ/T 221-2010) and combined with actual engineering application conditions. The volume fractions of steel fibers were set as 0%, 0.3%, 0.6%, 0.9%, and 1.2%. Ten test groups were designed, with steel fiber parameters summarized in Table 3.

Mixings were performed using an HJW-30/60 single horizontal shaft forced-action concrete mixer. Initially, steel fibers and fine stones were added and dry-mixed for 30 seconds. Subsequently, fine sand, river sand, and cementitious materials were incorporated and dry-mixed for an additional 30 seconds. Half of the premixed water and superplasticizer solution was added and mixed for 30 seconds, followed by the gradual addition of the remaining half and mixing for 60 seconds until homogeneity was achieved. After pouring, the specimens were not vibrated. The molds were released after 24 hours at ambient temperature and transferred to a curing chamber for 28 days, after which mechanical tests were conducted.

Table 2. The proportion of mixture for C50 self-compacting concrete (unit: kg/m^3)

Cement	Fine sand	River sand	Fine crushed stone	Water	Ground granulated blast furnace slag (GGBS)	Fly as
422	385	386	836	170	91	91

Table 3. Design parameters for specimen grouping

Volume fraction of steel fibers (%)	Length of steel fibers(mm)	Diameter of steel fibers(mm)
0	0	0
0.3	30	0.70
0.6	30	0.70
0.9	30	0.70
1.2	30	0.70
0.9	25	0.80
0.9	30	0.80
0.9	35	0.80
0.9	35	0.70
0.9	35	0.55

2.3 Test methods

2.3.1 Splitting Tensile Tests

The tensile strength was indirectly determined via the Brazilian splitting test. Test specimens were cylinders with a diameter of 100 mm and a height of 100 mm, four replicate tests were conducted for each condition. As depicted in Fig. 2, displacement-controlled loading was applied at a rate of 0.2 mm/min using an IRSM-RC-1500 rock/concrete uniaxial compression-shear apparatus.

(a) (b)

Fig. 2. Brazilian disc specimen (BD) (a) Front and (b) Vertical

2.3.2 NSCB Tests

As shown in Fig. 3, NSCB semi-cylinder specimens were configured with a radius (R) of 50 mm and a thickness (B) of 50 mm [20,21]. The notch length (a) was 20 mm, and the width (c) was 1.5 mm. Displacement-controlled loading was applied at 0.2 mm/min using a universal testing machine, with a support span (s) of 80 mm, five replicate tests were conducted for each condition.

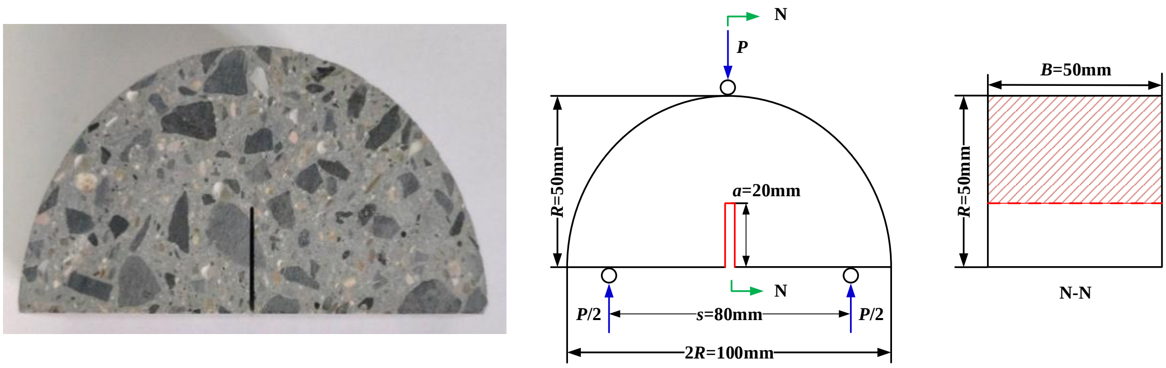

(a) (b)

Fig. 3. Notched semi-circular bend specimen (NSCB) (a) Physical and (b) Diagram

3. Results and Analysis

3.1 Brazilian Splitting Tests

3.1.1 Experimental Results

Owing to space limitations, Fig. 4 presents partial load-displacement curves of SCC under Brazilian splitting tests with varying steel fiber lengths, diameters, and volume fractions. As illustrated in Fig. 4, plain concrete exhibits a rapid load drop after reaching the peak load, accompanied by instantaneous specimen fragmentation and complete loss of bearing capacity. In contrast, SFRSCC demonstrates a slight load reduction during loading, followed by a secondary ascending branch of the curve. The magnitude of this post-cracking strength recovery varies significantly with the fiber length, the diameter, and the volume fraction. Correspondingly, SFRSCC specimens retain substantial residual bearing capacity after crack initiation without catastrophic failure.

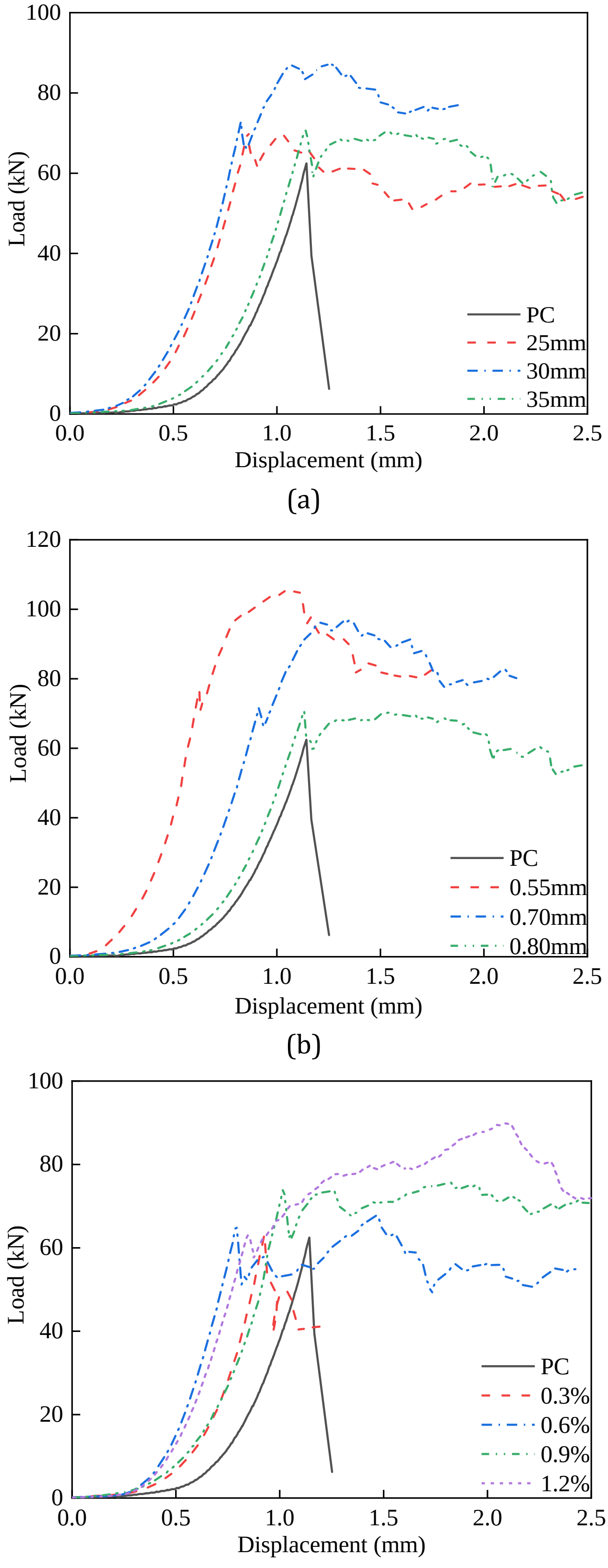

(c)

Fig. 4. Load-displacement curves of SFRSCC in the Brazilian splitting test(a) Influence of lengths (D=0.8mm, V_f=0.9%), (b) Influence of diameters (L=35mm, V_f=0.9%) and (c) Influence of volume fractions (L=30mm, D=0.7mm)

Specifically, when the volume fraction and diameter of steel fibers remain constant, the secondary ascending amplitude of the load-displacement curve obtained from the Brazilian splitting test first increases and then decreases with the increase in steel fiber length. The maximum secondary ascending amplitude appears at a fiber length of 30 mm. Compared with 25 mm fibers, 30 mm fibers provide a longer anchorage length, ensuring a strong bond between fibers and the matrix. However, when the fiber length is increased to 35 mm, the excessive length tends to cause uneven dispersion in concrete. Many fibers cannot effectively participate in load bearing, and local fiber agglomeration weakens the strength of the matrix, resulting in a lower secondary ascending amplitude of the load-displacement curve. When the length and volume fraction of steel fibers are unchanged, the secondary ascending amplitude of the load-displacement curve decreases continuously with the increase in fiber diameter. The largest secondary ascending amplitude is achieved at a fiber diameter of 0.55 mm. Under the same volume fraction, smaller diameter corresponds to a greater number of fibers, which can form a denser and more uniform crack-bridging network across the crack surface and thus exhibit better cooperative performance. When the length and diameter of steel fibers are kept constant, the secondary ascending amplitude of the load-displacement curve increases continuously with the increase in fiber volume fraction. A higher volume fraction enhances the fiber density in the cracked zone and reduces the average spacing between fibers. More fibers contribute to crack resistance, provide higher pull-out resistance and greater fracture energy. The combined effect of these factors leads to a continuous increase in the secondary ascending amplitude of the load-displacement curve after cracking [22].

3.1.2 The tensile Strength

Owing to space limitations, Fig. 5 illustrates the effect of steel fiber length on the tensile strength of SCC. Under conditions of fiber diameter (0.8 mm) and volume fraction (0.9%), the tensile strength initially increased and then decreased with increasing fiber lengths. The maximum tensile strength was observed at the fiber length of 30 mm, with a mean tensile strength enhancement of 24.3% compared to plain concrete. When the fiber length was 25 mm, the shorter embedment length on both sides of the splitting cracks led to easier fiber pull-out during tensile loading. Conversely, excessive fiber length (35 mm) reduced the number of fibers across the fracture plane, diminishing crack-arresting efficiency.

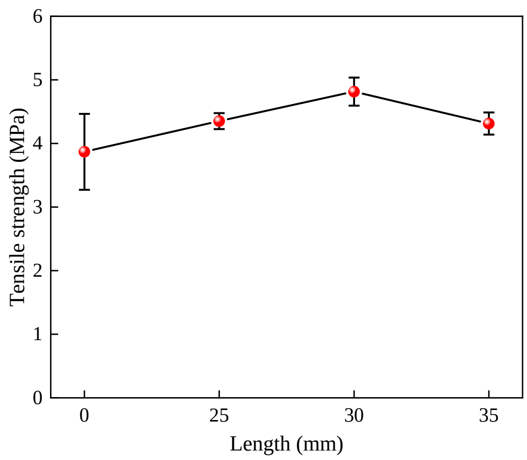

Fig. 5. Effects of steel fiber length on tensile strength of SFRSCC (D=0.8mm, V_f =0.9%)

Fig. 6 demonstrates the influence of steel fiber diameter on SCC tensile strength. With fixed fiber length (35 mm) and volume fraction (0.9%), tensile strength exhibited a parabolic trend, peaking at a diameter of 0.70 mm (30.23% increase vs. plain concrete). This optimal behavior is attributed to the larger specific surface area of 0.70-mm fibers, enhancing mechanical interlocking with the matrix for superior stress transfer. However, when the fiber diameter increased to 0.80 mm, the tensile strength began to decrease. This may be attributed to the change in fiber number and bonding characteristic between fiber and matrix under the same volume fraction. Larger diameter reduces the total number of fibers per unit volume, which weakens the crack arresting effect and stress distribution mechanism, thereby leading to the decline of tensile properties.

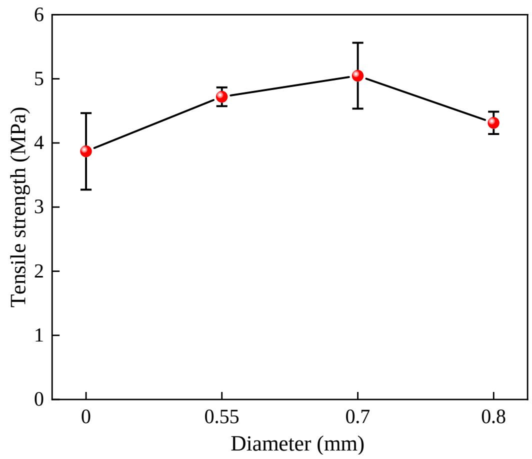

Fig. 6. Effects of steel fiber diameter on tensile strength of SFRSCC (L=35mm, V_f =0.9%)

Fig. 7 presents the effect of steel fiber volume fraction (V_f) on tensile strength. The tensile strength initially increased with V_f but decreased beyond 0.9%, at which point a maximum tensile strength enhancement of 12.1% was achieved. At this optimal volume fraction, steel fibers were uniformly dispersed in the matrix, which effectively bridged microcracks and retarded the propagation of macrocracks without significantly impairing workability. In contrast, when V_f reached 1.2%, fiber agglomeration restricted the flow of cement paste, resulting in internal voids and weak interfacial zones, thereby reducing the tensile strength [23,24].

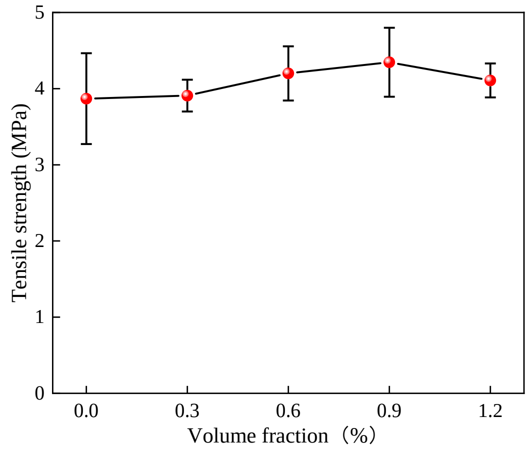

Fig. 7. Effects of steel fiber volume fraction on tensile strength in SFRSCC (L=30mm, D=0.7mm)

3.2 NSCB Tests

3.2.1 Experimental Results

Fig. 8 depicts representative load-displacement curves from NSCB tests under varying fiber parameters. Plain concrete and low-fiber specimens (V_f=0.3%) exhibited abrupt load drops post-peak, indicating a complete loss of bearing capacity. In contrast, higher V_f specimens displayed distinct post-cracking behavior.

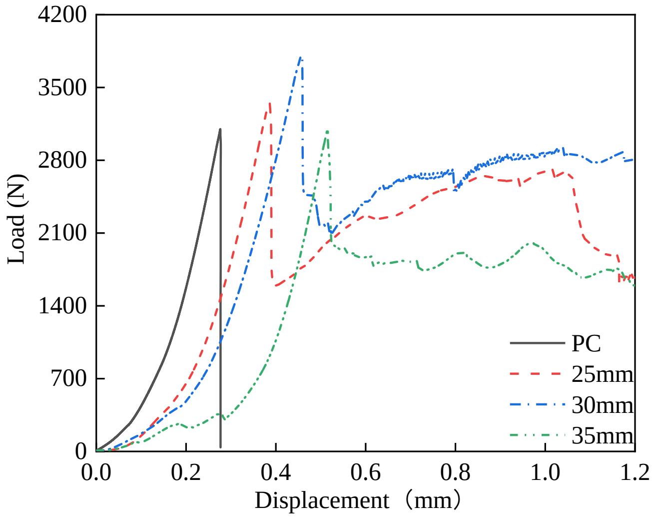

(a)

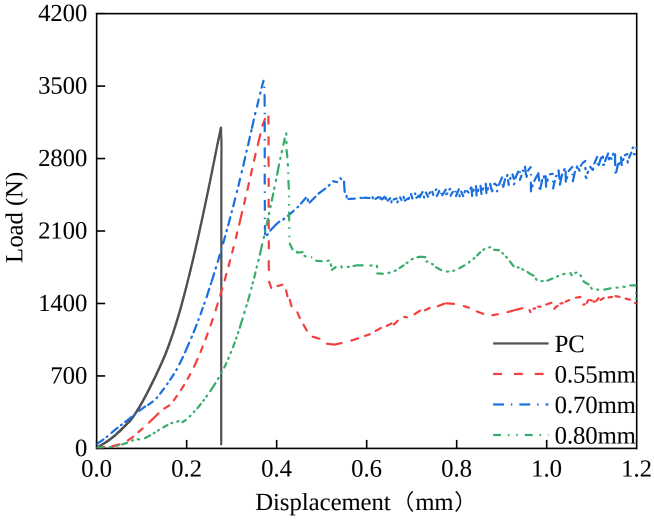

(b)

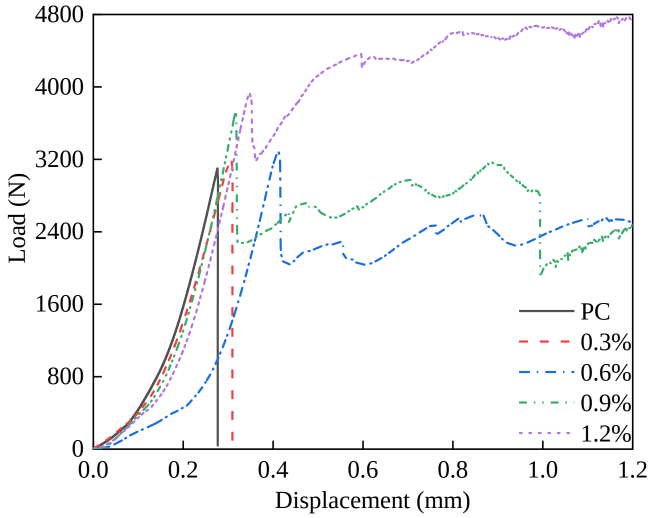

(c)

Fig. 8. Load-displacement curves of NSCB specimens in SFRSCC (a) Influence of lengths (D=0.80mm, Vf =0.9%), (b) Influence of diameters (L=35mm, V_f =0.9%) and (c) Influence of volume fractions (L=30mm, D=0.7mm)

The stable bearing phase (0.6%-0.9%V_f): After the initial cracking, loads stabilized below the critical level with flattened curves. Notably, the curve morphology showed a minimal sensitivity to the fiber geometry (L=25-35 mm, D=0.55-0.80 mm), confirming that the volume fraction dominates the post-cracking behavior over geometric parameters. The fiber bridging and stress redistribution delayed the failure [9], though V_f=0.6% provided only partial crack restraints. The strengthening phase (1.2% V_f): Specimens demonstrated the post-cracking strength recovery, surpassing the critical load via 3D fiber networks that transferred the stress through pull-out mechanisms. Reducing fiber spacings dispersed crack-tip stresses [25], activating broader matrix participation, and macroscopic load resurgence.

For self-compacting concrete (SCC), the residual bearing capacity not only reflects the toughness and energy absorption capacity of the material, but also reveals the improvement effect of internal crack propagation, interface bonding, and fiber bridging on the mechanical properties after damage. Referring to Reference [26] and combining with the NSCB load-displacement curves of SFRSCC in Fig. 8, the load corresponding to a post-peak displacement of 0.9 mm was selected as the residual bearing capacity, and the statistical results are shown in Table (4~6). It can be seen from Table (4~6) that: when the steel fiber diameter is 0.70 mm and the length is 30 mm, the residual bearing capacity of SCC after the NSCB test increases continuously with the increase in steel fiber volume fraction; when the steel fiber diameter is 0.80 mm and the volume fraction is 0.90%, the residual bearing capacity of SCC after the NSCB test first increases and then decreases with the increase in steel fiber length; when the steel fiber length is 35 mm and the volume fraction is 0.90%, the residual bearing capacity of SCC after the NSCB test first increases and then decreases with the increase in steel fiber diameter.

Table 4. Effect of steel fiber volume fraction on residual bearing capacity of self-compacting concrete after NSCB test

Volume fraction of steel fibers(%)	Length of steel fibers(mm)	Diameter of steel fibers(mm)	residual bearing capacity(kN)
0.30	30	0.70	0
0.60	30	0.70	2.50
0.90	30	0.70	2.82
1.20	30	0.70	4.60

Table 5. Effect of steel fiber length on residual bearing capacity of self-compacting concrete after NSCB test

Volume fraction of steel fibers(%)	Length of steel fibers(mm)	Diameter of steel fibers(mm)	residual bearing capacity(kN)
0.90	25	0.80	2.61
0.90	30	0.80	2.79
0.90	35	0.80	1.80

Table 6. Effect of steel fiber volume fraction on residual bearing capacity of self-compacting concrete after NSCB test

Volume fraction of steel fibers(%)	Length of steel fibers(mm)	Diameter of steel fibers(mm)	residual bearing capacity(kN)
0.90	35	0.55	1.30
0.90	35	0.70	2.61
0.90	35	0.80	1.90

Fig. 9 quantifies residual bearing capacities. Plain and low-fiber specimens fractured catastrophically along the notch, reflecting the brittle failure. With increased fiber parameters, cracks propagated tortuously above the notch (Fig. 9), as aggregates and fibers altered crack paths. Longer/larger fibers intensified crack deflection, increasing the fracture surface irregularity due to the impeded crack advancement.

(a) PC

(b) L=30mm, D=0.70mm, V_f=0.3%

(c) L=30mm, D=0.70mm, V_f= 0.6%

(d) L=30mm, D=0.70mm, V_f=0.9%

(e) L=30mm, D=0.70mm, V_f=1.2%

(f) L= 35mm, D=0.55mm, V_f= 0.9%

(g) L=35mm, D=0.70mm, V_f=0.9%

(h) L=35mm, D=0.80mm, V_f=0.9%

(i) L=25mm, D=0.80mm, V_f=0.9%

(j) L=30mm, D=0.80mm, V_f=0.9%

Fig. 9 Residual load-bearing capacity of NSCB specimens in SFRSCC

3.2.2 The Fracture Toughness

The stress intensity factor K serves as a metric for a material's resistance to crack propagation [20]. It is governed by factors such as applied stress, crack geometry, and dimensions. Research indicates that when K reaches a critical value, unstable crack propagation occurs. This critical value is termed the fracture toughness K_{IC} [21], which represents one of the fundamental fracture parameters in concrete fracture analysis and characterizes the material's crack resistance. According to the ISRM-recommended method, the Mode-I fracture toughness can be calculated using the formula proposed by Kuruppu et al [20]:

$$K_{Ic} = Y' \frac{P_{max}\sqrt{\pi a}}{2RB} \tag{1}$$

where K_{IC} is the stress intensity factor at crack initiation (i.e., fracture toughness), in MPa·m$^{1/2}$; P_{max} is the critical load at crack propagation (hereafter termed "critical load"), in kN; a is the notch length (20 mm); B is the specimen thickness (50 mm); R is the specimen radius (50 mm); Y' is the dimensionless stress intensity factor for Mode-I loading, expressed as:

$$Y' = -1.297 + 9.516\,(s/2R) - (0.47 + 16.457\,(s/2R))\beta + (1.071 + 34.401\,(s/2R))\beta^2 \tag{2}$$

where s is the span between the two supporting cylinders (80 mm); $\beta = a/R$, with $a = 20$mm, yielding β=0.4. Substituting the dimensions of the SCB specimen into Eq. (2) gives Y'=5.436248. Using Eq. (1), the fracture toughness K_{IC} of self-compacting concrete (SCC) NSCB specimens with varying steel fiber characteristic parameters was calculated, as illustrated in Fig. 10.

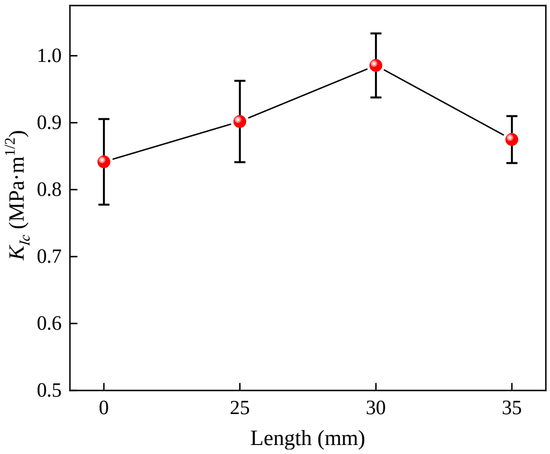

(a)

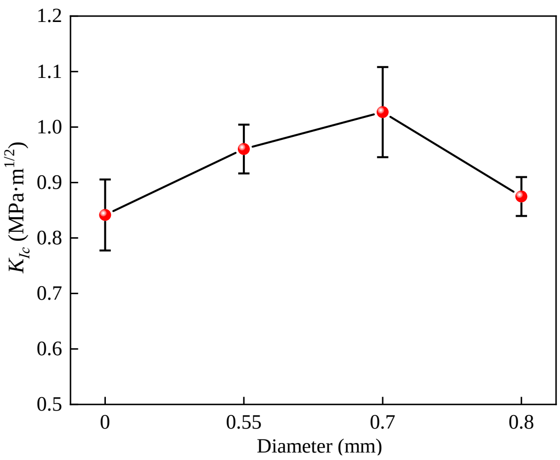

(b)

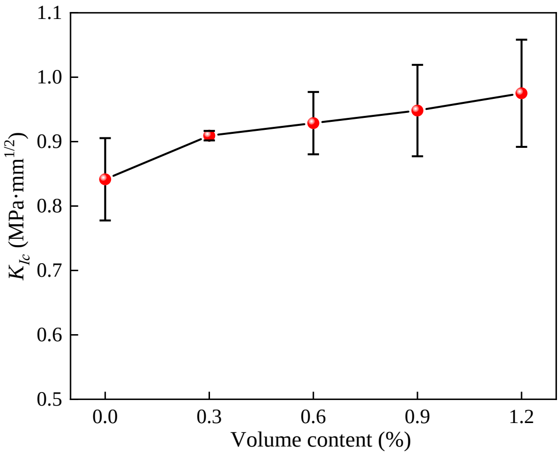

(c)

Fig. 10. Effects of steel fibers on the fracture toughness of SFRSCC (a) Influence of lengths (D=0.8mm, V_f =0.9%), (b) Influence of diameters (L=35mm, V_f =0.9%) and (c) Influence of volume fractions (L=30mm, D=0.7mm)

Fig. 10(a-b) reveals that the fracture toughness of SCC initially increases and then decreases with increasing steel fiber length and diameter. Specifically, when other fiber parameters are held constant, the maximum enhancement in fracture toughness (17.11%) relative to plain concrete occurs at a fiber length of 30 mm. The greatest improvement (22.03%) is achieved at a fiber diameter of 0.70 mm. Fig. 10(c) demonstrates a significant positive correlation between K_{IC} and V_f, at V_f=0.3%, K_{IC}=0.91MPa • m$^{1/2}$, and an 8.33% increase over plain concrete (0.84 MPa • m$^{1/2}$). Further increases in V_f, K_{IC} continue to elevate, when V_f=0.6%, K_{IC}=0.93 MPa • m$^{1/2}$ (+10.71%), when V_f=0.9%, K_{IC}=0.94 MPa • m$^{1/2}$(+12.00%), and when V_f=1.2%, K_{IC}=0.97 MPa • m$^{1/2}$ (+15.48%). During the NSCB test of SFRSCC specimens, crack propagation leads to the pull-out of steel fibers from the matrix. The pull-out process requires overcoming the interfacial bond strength and friction between the fibers and the matrix. Owing to its excellent fluidity, self-compacting concrete forms a denser and more uniform interfacial transition zone with steel fibers, which improves the bond performance between fibers and the matrix [27]. This enables SFRSCC to dissipate more energy during the fracture process, thereby enhancing its fracture toughness.

It can be seen from the test results that the variation law of fracture toughness of steel fiber-reinforced self-compacting concrete (SFRSCC) with steel fiber volume fraction, length, and diameter is basically consistent with that of residual bearing capacity in Section 3.2.1. Specifically, both the fracture toughness and residual bearing capacity of SFRSCC increase continuously with the increase in steel fiber volume fraction. With the increase in steel fiber diameter, both increase first and then decrease. Similarly, with the increase in steel fiber length, both also show a trend of increasing first and then decreasing.

It is worth noting that the tensile strength and fracture toughness exhibit different variation trends at high fiber volume fractions. When the volume fraction exceeds 0.9%, the tensile strength decreases, whereas the fracture toughness continues to increase even at 1.2%. The main reason for this difference is as follows: Tensile strength is an overall mechanical index that is highly sensitive to the compactness, uniformity, and internal defects of concrete. Excessive fiber content tends to deteriorate workability and increase internal pores and weak interfaces, thereby reducing the tensile strength [28]. In contrast, fracture toughness mainly depends on the crack bridging, crack resistance, and energy dissipation of fibers after crack initiation. Even at a high volume fraction, the increased number of fibers can still provide sufficient bridging stress and toughening effect during crack propagation.

3.3 Correlation Analysis of The Tensile Strength and The Fracture Toughness

The failure of steel fiber-reinforced concrete (SFRC) originates from the propagation of microcracks under tensile stress. The fracture toughness quantifies the material's intrinsic resistance to crack propagation and correlates with the mechanical strength. Numerous studies [17, 29-34] have established a linear relationship between Mode-I fracture toughness (K_{Ic}) and tensile strength (σ_t) for materials like rock, clay, and concrete (Table 7).

Table 7. Compilation of empirical correlations between K_{Ic} and σ_t

Data source	Material category	Empirical formula
Su et al. [17]	Steel Fiber-Reinforced Reactive Powder Concrete	σ_t =1.76 K_{Ic}+4.30
Yang et al. [29]	Coal	σ_t =5.48K_{Ic}
Deng et al. [30]	Sandstone	σ_t=8.32K_{Ic}
Wang et al. [31]	Clay	σ_t =2.82K_{Ic}
Zhang [32]	Rock	σ_t =6.88K_{Ic}
Ding et al. [33]	Steel fiber-reinforced recycled concrete	σ_t =4.44K_{Ic}+0.86
Liu et al. [34]	Plastic concrete	σ_t =2.28K_{Ic}

Given that concrete aggregates derive from crushed natural rocks, the relationship between K_{Ic} and σ_t for SFRC was investigated. Linear regression of experimental data (Fig. 11) yields.

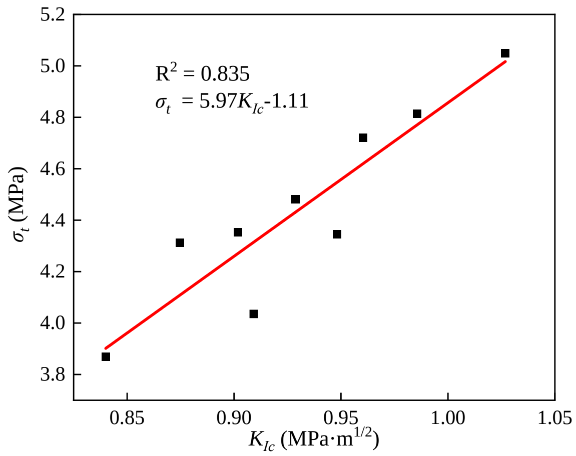

Fig. 11. Correlations between tensile strength (σt) and fracture toughness (KIc) of SCC with varied steel fiber parameters

σ_t is determined from the splitting tensile strength of cylindrical specimens, while K_{Ic} describes the resistance to rapid crack propagation in NSCB specimens. Both parameters reflect tensile performance but differ in focus: K_{Ic} emphasizes the resistance to crack propagation, whereas σ_t measures the global maximum load-bearing capacity. Given the simplicity of the Brazilian splitting test compared to fracture toughness tests, this linear correlation facilitates the prediction of K_{Ic} for SFRC.

4. Conclusions

- After incorporation of steel fibers, the concrete specimens do not experience complete fracture upon the occurrence of splitting cracks. The load-displacement curves show a slight stress drop, but the bearing capacity continues to increase with further loading. Such an increase is closely related to fiber length, diameter, and volume fraction.
- The tensile strength of self-compacting concrete (SCC) first increases and then decreases with increasing steel fiber length, with the maximum average tensile strength obtained at a fiber length of 30 mm. Similarly, the tensile strength increases initially and then decreases

with increasing fiber diameter, reaching the peak value at 0.70 mm. With increasing steel fiber volume fraction, the tensile strength rises first and then declines, and the optimal strengthening effect is achieved at a volume fraction of 0.9%.

- The load-displacement curves of steel fiber-reinforced self-compacting concrete (SFRSCC) obtained from NSCB tests exhibit a brief stress reduction during initial crack propagation, followed by a secondary load-bearing stage. The mechanical behavior in this stage is more significantly affected by the steel fiber volume fraction than by fiber length or diameter. At volume fractions of 0.6% and 0.9%, the specimens retain bearing capacity below the cracking load after initial cracking, and the curves gradually flatten. At a volume fraction of 1.2%, the bearing capacity not only resists degradation after initial cracking but also continues to increase beyond the critical load.
- The fracture toughness of SCC first increases and then decreases with increasing steel fiber length and diameter. Under the condition that other fiber parameters remain unchanged, the maximum improvement in fracture toughness (relative to plain concrete) is achieved at a fiber length of 30 mm and a fiber diameter of 0.70 mm. The fracture toughness shows a clear increasing trend with rising steel fiber volume fraction, reaching the optimal enhancement at 1.2%.
- Based on the experimental data for SFRSCC, a statistically robust linear relationship exists between the tensile strength (σ_t) and the mode-I fracture toughness (K_{IC}). The constitutive equation is formulated as: $\sigma_t = 5.97K_{Ic}$-1.11, with a coefficient of determination (R^2 = 0.835), confirming a strong correlation.

Acknowledgments

This work was supported by the Fundamental Research Funds for the Central Universities of North Minzu University (No. 2023ZRLG16) and the Anhui Provincial Natural Science Foundation (No. 2308085QE194).

References

[1] Traver-Abella C, Bonet JL, Miguel PF, et al. Effect of steel fibres on the shear behaviour of SCC dry joints in precast segmental bridges. Constr Build Mater, 2024; 415: 134998. https://doi.org/10.1016/j.conbuildmat.2024.134998

[2] Karuppasamy M, Balakrishnan B, Chandran K, et al. Analysis of mechanical properties in self-compacting concrete enhanced with steel fibers. Micro Nano Lett, 2024; 19(4): e12203. https://doi.org/10.1049/mna2.12203

[3] Pour AK, Shirkhani A, Noroozinejad Farsangi E. Effect of high-range water reducer and W/C ratio on the fresh and mechanical properties of fiber-reinforced natural zeolite SCC. Struct Concr, 2024; 25(5): 4075 - 4102. https://doi.org/10.1002/suco.202301071

[4] Mousavi SR, Afshoon I, Bayatpour MA, et al. Effect of waste glass and curing aging on fracture toughness of self-compacting mortars using ENDB specimen. Constr Build Mater, 2021; 282: 122711. https://doi.org/10.1016/j.conbuildmat.2021.122711

[5] Zhao Y, Bi J, Sun Y, et al.Synergetic effect of ground granulated blast-furnace slag and hooked-end steel fibers on various properties of steel fiber reinforced self-compacting concrete. Struct Concr, 2022; 23(1): 268 - 284. https://doi.org/10.1002/suco.202000722

[6] Abbas S, Soliman AM, Nehdi ML. Exploring mechanical and durability properties of ultra-high performance concrete incorporating various steel fiber lengths and dosages. Constr Build Mater, 2015; 75: 429 - 441. https://doi.org/10.1016/j.conbuildmat.2014.11.017

[7] Shi X, Park P, Rew Y, et al. Constitutive behaviors of steel fiber reinforced concrete under uniaxial compression and tension. Constr Build Mater, 2020; 233: 117316. https://doi.org/10.1016/j.conbuildmat.2019.117316

[8] Chen CC, Wu ZM, Hu X, et al. Influence of fiber shape and curing system on strength and toughness of UHPC. Materials Repoerts, 2024, 38(15): 139-149.

[9] Ning XL, Ding YN. Experimental research on crack width of steel fibers reinforced self-consolidating concrete beams. Eng Mech, 2017; 34(4): 116 - 122.

[10] Liu RY, Wang ZJ. Research on crack development of unreinforced steel fiber concrete compression-bending. Build Struct, 2020; 50(22): 93 - 93.

[11] Han JP, Han WL, Wen XH, et al. Experimental investigation on the influence of steel fiber on the workability and compressive toughness of self-compacting concrete. J Lanzhou Univ Technol, 2024; 50(5): 112 - 117.
[12] Li J, Hu HN. Mechanical properties and pore structure characteristics of fiber reinforced self-compacting concrete. Acta Mater Compos Sin (Online First). Accessed 2025-06-06.
[13] Ola AQ. High temperature effect on shear transfer strength of steel fiber reinforced self-compacted concrete. J Eng Appl Sci, 2019; 14(10): 3158 - 3174. https://doi.org/10.36478/jeasci.2019.3158.3174
[14] MUSA A M. Robustness of self consolidating steel fiber reinforced concrete[J]. 2009.
[15] Hafez B, Glusac J, Aslani F. Re-centring and flexural toughness performance of novel steel fibre-reinforced self-compacting concrete. International Journal of Concrete Structures and Materials, 2025, 19(1): 90. https://doi.org/10.1186/s40069-025-00836-7
[16] Ayatollahi MR, Mahdavi E, Alborzi MJ, et al. Stress intensity factors of semi-circular bend specimens with straight-through and chevron notches. Rock Mech Rock Eng, 2016; 49: 1161 - 1172. https://doi.org/10.1007/s00603-015-0830-y
[17] Su C, Wu Q, Weng L, et al. Experimental investigation of mode I fracture features of steel fiber-reinforced reactive powder concrete using semi-circular bend test. Eng Fract Mech, 2019; 209: 187 - 199. https://doi.org/10.1016/j.engfracmech.2019.01.029
[18] Razmi A, Mirsayar MM. On the mixed mode I/II fracture properties of jute fiber-reinforced concrete. Constr Build Mater, 2017; 148: 512 - 520. https://doi.org/10.1016/j.conbuildmat.2017.05.034
[19] Zhang J, Sakhaeifar MS, Little DN, et al. Characterization of crack growth rate of sulfur-extended asphalt mixtures using cyclic semicircular bending test. J Mater Civ Eng, 2018; 30(12): 04018311. https://doi.org/10.1061/(ASCE)MT.1943-5533.0002517
[20] Kuruppu MD, Obara Y, Ayatollahi MR, et al. ISRM-suggested method for determining the mode I static fracture toughness using semi-circular bend specimen. Rock Mech Rock Eng, 2014; 47: 267 - 274. https://doi.org/10.1007/s00603-013-0422-7
[21] Aziminezhad M, Mardi S, Hajikarimi P, et al. Loading rate effect on fracture behavior of fiber reinforced high strength concrete using a semi-circular bending test. Constr Build Mater, 2020; 240: 117681. https://doi.org/10.1016/j.conbuildmat.2019.117681
[22] Kosior-Kazberuk M, Krassowska J. Fracture behaviour of basalt and steel fibre reinforced concrete. Budownictwo i Inżynieria Środowiska, 2015, 6(2).
[23] Jin QP, Chen C, Huang QL, et al. Review on the Effects of fiber action in ultra high-performance concrete. J Water Resour Archit Eng, 2024; 22(2): 55 - 65.
[24] Ma QY, Zhang HP, Li LY, et al. Compressive-tensile properties and hybrid effect of fiber reinforced self-compacting concrete. J Anhui Univ Technol Nat Sci, 2022; 39(3): 317 - 326.
[25] Ma YD, Ma KZ, Liu BQ. Analysis of shear bearing capacity of hybrid steel fiber reinforced concrete deep beams. J Harbin Inst Technol, 2022; 54(3): 95 - 107.
[26] Oettel V, Schulz M, Haist M. Empirical approach for the residual flexural tensile strength of steel fiber-reinforced concrete based on notched three-point bending tests[J]. Structural Concrete, 2022, 23(2): 993-1004. https://doi.org/10.1002/suco.202100565
[27] Cunha V M C F, Barros J A O, Sena-Cruz J M. Pullout behavior of steel fibers in self-compacting concrete. Journal of Materials in Civil Engineering, 2010, 22(1): 1-9. https://doi.org/10.1061/(ASCE)MT.1943-5533.0000001
[28] Guo YD, Liu YZ, Wang WJ, et al. Influence of basalt fiber characteristic parameters on uniaxial tensile properties of concrete[J]. Acta Materiae Compositae Sinica, 2023, 40(5): 2897-2912.
[29] Yang L, Li JZ, Lou JF, et al. Study on fracture characteristics of coal samples based on notched semi-circular bending tests. J Min Saf Eng, 2022; 39(5): 1041 - 1050.
[30] Deng HF, Zhu M, Li JL, et al. Study of mode-I fracture toughness and its correlation with strength parameters of sandstone. Rock Soil Mech, 2012; 33(12): 3585 - 3591.
[31] Wang JJ, Zhu JG, Chiu CF, et al. Experimental study on fracture toughness and tensile strength of a clay. Eng Geol, 2007; 94(1-2): 65 - 75. https://doi.org/10.1016/j.enggeo.2007.06.005
[32] Zhang ZX. An empirical relation between mode I fracture toughness and the tensile strength of rock. Int J Rock Mech Min Sci, 2002; 39(3): 401 - 406. https://doi.org/10.1016/S1365-1609(02)00032-1
[33] Ding YH, Zou CL, Guo M, et al. Mechanical and fracture properties of steel fiber reinforced concrete with large amount of recycled aggregate. Bull Chin Ceram Soc, 2023; 42(7): 2532 - 2540.
[34] Liu GH, Gan L, Liu Y, et al. Effect of different sand ratio and aggregate sizes on fracture toughness of plastic concrete. Adv Sci Technol Water Resour, 2024; 44(3): 39 - 44 + 87.